



Case study and numerical modelling of heat transfer in a snow-covered building roof



Borui Zhang ^{a,b}, Qingwen Zhang ^{a,b,*}, Huamei Mo ^{a,b,**}, Feng Fan ^{a,b}

^a Key Lab of Structures Dynamic Behavior and Control of the Ministry of Education, Harbin Institute of Technology, Harbin, 150090, China

^b Key Lab of Smart Prevention and Mitigation of Civil Engineering Disasters of the Ministry of Industry and Information Technology, Harbin Institute of Technology, Harbin, 150090, China

ARTICLE INFO

Keywords:

Heat transfer

Snow on roof

Field measurements

Temperature-dependent constitutive model

FEM

ABSTRACT

We explored the heat transfer in a snow-covered building roof by setting a prototype field measurement in Harbin during the winter of 2018. Several sets of data were measured, including the meteorological elements and snow properties. Hence, a temperature-dependent constitutive model for a heterogeneous medium, the deposited snow on the roof, was accordingly proposed. To validate this, this model was adopted in a new proposed 3-D finite element modelling (FEM), in ANSYS software, to quantitatively analyze the heat transfer process. All heat transfer patterns, including roof heat-loss conduction, surrounding turbulent exchange, and net radiation, as well as the involved phase-changes in snow metamorphism, were considered. Using the birth and death element technique, the snowmelt and subsequent ice-layer formation can also be visually reproduced. The feasibility of the FEM was validated by comparing both the snow metamorphic features and the hourly temperature gradient in the snow between the FEM and the prototype measurement. In future work, the influence of water vapor transport in snow and the range of time-scales should be increased in further studies.

1. Introduction

Building designs are, in part, the product of human adaptation to climate. With the high occurrence of extreme climates in recent years, the influence of snowfalls and snowdrifts on and around building in snowy regions has received attention from research workers worldwide. Herein, the influence of heat loss through building roofs on deposited snow-layers is one of the important branches in this field. Yet many direct damages and indirect disasters, including ice-dam formation and falling, ceiling and wall leakage, rooftop avalanches, and even roof collapse, have occurred in the snow-covered buildings due to unreasonable strategies for building heating in winter [1,2].

To avoid such disasters, a quantified coefficient (the thermal coefficient C_t) for the modification of snow-load has been accordingly put forward in several national codes [3,4]. But it should be stressed that, the available data for coefficient determination can only cover limited field measurements [5–8], and its accuracy highly depends on the number of observations. However, the monitoring and analysis of heat transfer and resulting snow metamorphism in a snow-covered roof have rarely been investigated. Those relevant works [9,10] are still in the exploratory stage, mainly consulting on the relative mathematical methods [11,12] or hydrology models [13,14],

* Corresponding author. Key Lab of Structures Dynamic Behavior and Control of the Ministry of Education, Harbin Institute of Technology, Harbin, 150090, China.

** Corresponding author. Key Lab of Structures Dynamic Behavior and Control of the Ministry of Education, Harbin Institute of Technology, Harbin, 150090, China.

E-mail addresses: zhangqw@hit.edu.cn (Q. Zhang), mohuamei@hit.edu.cn (H. Mo).

<https://doi.org/10.1016/j.csite.2022.102248>

Received 19 September 2021; Received in revised form 16 June 2022; Accepted 25 June 2022

Available online 4 July 2022

2214-157X/© 2022 The Authors. Published by Elsevier Ltd. This is an open access article under the CC BY-NC-ND license (<http://creativecommons.org/licenses/by-nc-nd/4.0/>).

in which the pursuit of both the abundance and diversity of the mathematical expressions of the physical processes, like water infiltration and vapor transport, are the primary research missions. And they have possibly limited guidance role for providing the building snow-load assessment, or the snow heat transfer analysis, in the perspective of engineering application.

To consider this, in this study, a novel modelling strategy for heat transfer analysis in the snow-covered building roof has been put forward via the ANSYS software. Comparing to the widely-used CFD solidification and melting model (the Fluent software) in the relevant field, the potential snow morphological change and ice-layer formation, due to the metamorphism effects, can be visually reproduced using the birth and death element technique by APDL programming. To well describe the thermal properties of snow material, a simplified temperature-dependent constitutive model, based on the prototype record, has been established and adopted in this proposed 3-D finite element modelling (FEM). The feasibilities of the snow constitutive model and the FEM have been validated by comparing the simulated results, including multi-directional temperature gradients and fluctuations, with that of the on-site benchmark field measurement (case study) undertaken in Harbin, China.

2. FEM modelling strategy

2.1. Modelling hypothesizes and theory

Being similar to the thermal analysis in the traditional engineering field, such as the application of hybrid nanofluids [15], the problem solving of heat transfer mainly consists of two categories, including the directly theoretical calculation and the FEM modeling, where the latter is applied in this study. In theory, snow constitutes a heterogeneous system, namely the ice-water-air system, where it is usually assumed to be in local thermal equilibrium. To correctly simulate the heat transfer through snow, a model in the particle scale should be accordingly proposed in principle, but the low computational efficiency challenges the development of such a dispersed model. Instead, the deposited snow on the roofs, in the form of the aggregate of particles, can usually be simplified as a porous solid phase, the contribution of intergranular flow to convective heat can be neglected in practical application [16].

To visually reproduce the snow morphological change via the FEM, several hypothesizes proposed to simplify the heat transfer mechanism in the snow system: 1) Using the variation of apparent snow density to describe the porosity change, caused by the metamorphism effects; 2) Using an enthalpy method [17,18] to show the internal energy (sensible heat and latent heat) variations during the phase-change of snow, so that the energy balance equation can be formulated more concisely without further adjustment for the melting water; 3) Using the birth and death element technique to ‘kill’ the overheated ($0\text{ }^{\circ}\text{C}$) elements and ‘renew’ the ice elements at the end of each loading step to describe the snowmelt and ice formation. On the premise of those hypothesized sets, this study can provide insight into the achievement of the dynamic change of snow thermal properties in the heat transfer analysis, which differs from the existing FEM of inputting stationary parameters for the snow system [10,11].

Herein, the governing equation can be established based on an energy balance between the snow and surroundings, where the energy conservation is described in terms of the mixture enthalpy as:

$$\nabla \cdot (k_{\text{seff}} \nabla T) + S = \rho_s \frac{dH}{dt} \quad (1)$$

where k_{seff} is the effective thermal conductivity of snow; T is the snow temperature; ρ_s is the apparent snow density; t is the time; S is the source-term of the heat transfer in a snow-covered building roof, including heat from conduction, convection, and radiation; H is the volumetric heat enthalpy of snow which can be generally defined as follows [17]:

$$H = \int_{T_{\text{ref}}}^T C_p(T) dT + \omega_l(T)L \quad (2)$$

where the subscript ref presents the reference value in the standard state, thus T_{ref} is the reference temperature, $0\text{ }^{\circ}\text{C}$; C_p is the snow heat capacity; L is the latent heat of melting water; ω_l is the liquid component volume fraction of the snow, and these parameters both vary with temperature.

For the source-term S determination, the snow-layers on the building roof are fully exposed to the meteorological elements, and the ambient atmosphere or the co-current turbulent wind is forced to flow along with the snow-layers, forming an accompanying boundary layer to achieve the convection (Q_{conv}). The solar and atmospheric radiation (Q_{rad}) incident upon the free surface of the snow-layers is mostly transmitted across the snow and mainly absorbed by both the snow-layers and building roofs. Due to the installation of the building heating system, some partial indoor heat (Q_{cond}) can conduct upward to the ambient atmosphere across the snow-covered building roof without enough thermal insulation of the roof maintenance properties.

2.2. Heat conduction

Known as snow, a heterogeneous material, whose ‘effective’ heat conductivity is usually applied in calculating heat from conduction (Q_{cond}). This ‘effective’ property depends on the conductivities of snow fundamental constituents, and the contributions of water vapor phase change and diffusion should be included [19]. For practicability, in snow engineering, the effective thermal conductivity of snow is usually established and distinguished based on the snow’s apparent density and its crystal category [20,21]. In this study, a congruent relation between snow temperature and its effective thermal conductivity is established, where the apparent density of snow is taken as an intermediate variable, as illustrated in Eq. (3).

$$k_{\text{eff}} = \psi(\rho_s) \xrightarrow[\text{field-measurements}]{\rho_s = \varphi(T_s)} k_{\text{eff}} = \psi(\varphi(T_s)) \quad (3)$$

where k_{eff} is the effective thermal conductivity; T_s is the temperature of snow; ψ and φ represent the quantitative relationships between k_{eff} , ρ_s and T_s .

Moreover, considering that the deposited snow on the roof is in the form of the aggregate of particles, the non-tight contact between snow and roof surface cannot be ignored in such a dispersed system, so that a contact thermal conductivity k_c is also considered, where it can be estimated based on the theory of thermal contact conductance [22].

$$k_c = \frac{2k_{\text{eff}}k_{rs}}{k_{\text{eff}} + k_{rs}} \quad (4)$$

where k_c is the contact thermal conductivity between snow-layer and roof surface; k_{rs} is the thermal conductivity of the building roof.

2.3. Heat convection

In view of the calculation of convective heat (Q_{conv}), both the sensible (SHL) and latent (LHF) heat fluxes should be considered, meaning that turbulent transfer of heat towards or away from the snow surface. In detail, these sensible and latent heat fluxes, caused by turbulent wind exchange, can be conveniently estimated from bulk transfer relationships as follows [23]:

$$\begin{cases} \text{SHF} = \rho_a u C_p (T_s - T_a) \\ \text{LHF} = \rho_a u L_e C_e (E_s - E_a) \end{cases} \quad (5)$$

where ρ_a and C_p are the density and isobaric specific heat of air; L_e is the latent heat of snow sublimation, whose amount is equal to 2838 kJ/kg; u is the rate of the convective process (mean wind velocity); T and E are the potential temperature and relative humidity in the air at some specific height, subscripted a , and that of the snow surface, subscripted s , respectively; C_h and C_e are defined bulk transfer coefficients, empirically those parameters are assumed to be equal [24].

The heat transfer coefficients (C_h and C_e) can be estimated based on the principle of the boundary layer theory for plates [25]. In calculation, the fluid properties as well as flow conditions, including laminar and turbulent flow, are described by the Prandtl number P_r (a constant 0.71 for air) and the Reynolds number R_e ($\leq 5 \times 10^5$ for laminar flow and $\geq 5 \times 10^5$ for turbulent flow), respectively:

$$C_h, C_e = \begin{cases} 0.664 R_{el}^{1/2} P_r^{1/3} \frac{k_{\text{eff}}}{L} & \left\{ \begin{array}{l} \frac{k_{\text{eff}}}{L} (Re \leq 5 \times 10^5) \\ \frac{k_{\text{eff}}}{L} (5 \times 10^5 \leq Re \leq 10^8) \end{array} \right. \\ (0.037 R_{el}^{0.8} - 870) P_r^{1/3} \frac{k_{\text{eff}}}{L} & \end{cases} \quad (6)$$

where the subscript l represents laminar flow, and the subscript t represents turbulent flow; L is the characteristic scale of the snow; and the Reynolds number R_e that can be expressed as $Re = uL\rho_a/\mu$, herein, u is the mean wind velocity; and μ represents the viscosity coefficient of air.

2.4. Heat radiation

The radiative heat (Q_{rad}) contains two categories: solar short-wave radiation (S_{ssr}) and atmosphere long-wave radiation (S_{alr}). Those calculation in the FEM can be achieved based on the Dilger model [26], in which the intensity of direct solar radiation S_{ssr} on the snow-layers can be determined by:

$$S_{\text{ssr}} = 0.90^{mp} S_0 \left(1 + 0.034 \cos\left(\frac{2\pi N}{365}\right) \right) \cos \theta \quad (7)$$

where S_0 is the solar radiation without attenuation of the Earth's atmosphere, termed extra-terrestrial radiation; N is the day of the year (starting 1 for January 1st); θ is the solar incident angle between the normal of the snow-layer's surface and the sunlight; m is the atmospheric optical mass that can be determined by the relative air pressure and the solar altitude; p is the atmospheric turbidity. Then, based on the calculation method proposed by Threlkeld [27], the diffuse component can be estimated by a dimensionless parameter C , which is to describe the percent of diffuse radiation S_{sdr} accounts for S_{ssr} , according to the spherical triangulation and the concepts of astronomy. In terms of the albedo of the snow [28], the reflected component S_{srr} can be acquired based on the sum of S_{ssr} and S_{sdr} .

Except for the reflected solar radiation, the residual radiation penetration through the snow shows a significant non-linear characteristic. In detail, the atmosphere long-wave radiation S_{alr} absorbed in snow-layer can be quantified by Lambert's law [29]. Herein, the effective sky temperature T_{sky} is estimated by a fitting model [30], used for determining the longwave radiative heat absorbed in snow, in a form of:

$$S_{\text{alr}} = e_s \sigma \left(F_{sg} (T_{\text{ground}}^4 - T_s^4) + F_{ss} (T_{\text{sky}}^4 - T_s^4) \right) \quad (8)$$

where e_s is the surface longwave radiation emittance that can be ascertained from the dew-point temperature, usually about 0.85 for snow; σ is the Stefan-Boltzmann constant; F_{sg} is the coefficient to describe the angle between snow surface and ground; F_{ss} is the coefficient to describe the angle between snow surface and sky; T_{ground} , T_s and T_{sky} are the temperatures of the ground, snow and

effective sky, respectively.

2.5. Modelling technique

The schematic diagram of the FEM modelling technique is shown in Fig. 1. In detail, the first step is to ensure the initial FEM thermal boundaries based on the prototype meteorological elements. The next step is to establish a temperature-dependent snow constitutive model, where the kernel idea of this is to illustrate the dynamic changes of snow properties via the real-time fluctuant temperature. Herein, some empirical relations between snow temperature and other physical properties, namely apparent density, scale, and liquid component volume fraction, can be established in sequence.

Particularly, the temperature-enthalpy relation can be served as the reference for the snowmelt energy criterion in the enthalpy method (Eq. (3)). While the temperature-density relation is used for describing the porosity change, this can also be taken as an intermediate variable to express the fluctuation of snow-effective thermal conductivity with temperature (Eq. (2)). Then, the potential snow phase change, as well as three heat-transfer patterns are calculated based on the above theories. All element properties can be updated at the end of the current calculation step. In the case of snow element temperature above the melting point (0°C), the adoption of the birth and death element technique can realize the reproduction of the snowmelt and ice-layer formation on the roof surface. The ‘birth and death’ in modelling technique means that, the thermal properties of overheated snow elements ($\geq 0^{\circ}\text{C}$) can be replaced by that of water, called the newborn of water elements. Meanwhile, to simulate the melt-water percolation and refreezing in the gap between snow and roof surface, the thermal properties of contact elements (Eq. (4)) can be directly changed to the corresponding properties of ice, also called the newborn of ice elements.

Finally, the hourly temperature-field distribution of snow-layers in both horizontal and vertical directions can be acquired by several cyclic loading steps.

3. Case study: prototype field measurement

3.1. Layout of the case study site and data acquisition

To validate the feasibility of the FEM, a long-term field measurement was conducted on a heated building in Harbin during the winter of 2018. The study case site is located on the building roof of the school of civil engineering at Harbin Institute of Technology (HIT), northern China ($E126.69^{\circ}$, $N45.77^{\circ}$). Here the winter is the dominant season, usually with a large number of snowfalls. As shown in Fig. 2a, the test site is located on the tallest building in the locality. The building’s flat roof (with a 2% slope for water draining) is fully exposed to meteorological elements, namely wind, snow, solar radiation, etc.

Two 3×3 m areas of balanced snow-layers (with the same depth) were selected on the building roof after obvious snowfalls. One area was used for long-term snow temperature monitoring to observe the thermal performance of this snow-covered roof, whilst the other was used to determine the snow properties for the analytical parameters in the snow constitutive model applied in the FEM.

The measured database was established from the long-term recorded field data that contained two parts: 1) the meteorological elements and hourly snow properties, like apparent density, liquid water content, etc.; and 2) the heat transfer evaluation parameters, including snow temperature and heat flux.

In detail, the meteorological elements, including ambient air temperature, relative humidity, wind velocity and incoming solar

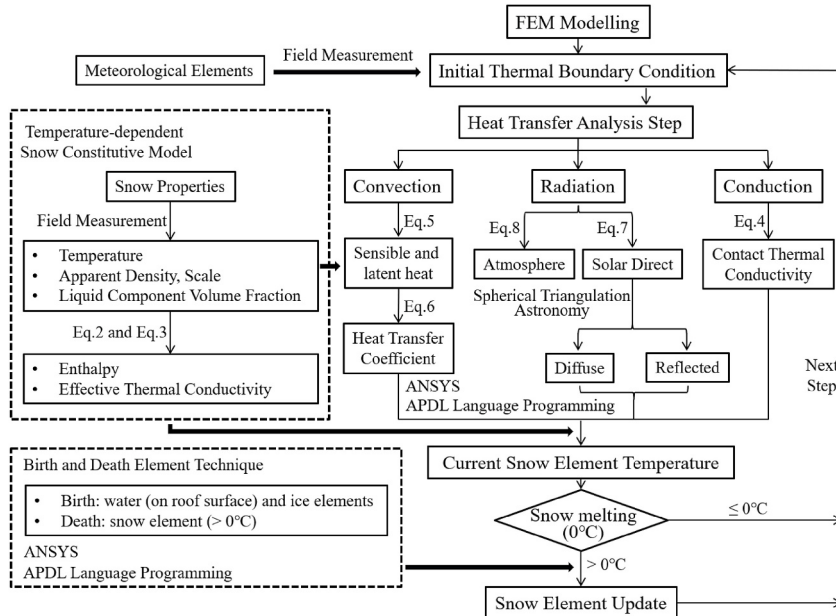


Fig. 1. Schematic diagram of the FEM modelling.

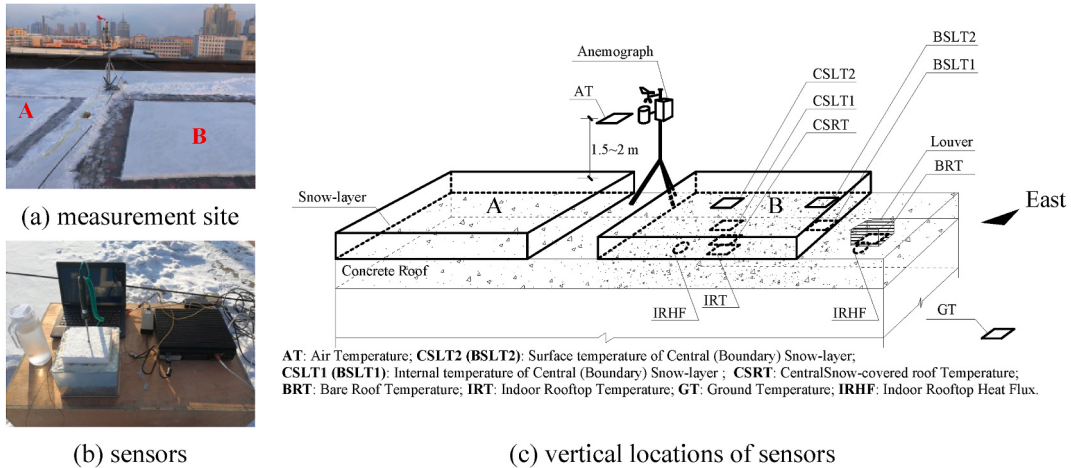


Fig. 2. Field measurement site and instrument arrangements.

radiation were acquired automatically by an anemograph (PC-6, Sunshine MTech, Inc) that was sited approximately 1.8 m above the building roof (Fig. 2a). Moreover, the apparent density of snow was acquired by measuring the sample's mass and snow-depth every hour, from 6 a.m. to midnight, using a snow gauge and an electronic balance with a resolution of 0.1 g. The snow temperature distribution was recorded by a wireless transmitting temperature sensor system (RC-4, Elitech, Inc), and the sampling frequency of the temperature sensor was set as 1min. To reasonably evaluate the liquid water content of snow, a calorimeter (Fig. 2b) was designed for the study to work with an FBG demodulator (SI255, MOA, Inc) according to the calorimetric method [31]. Since the thermal metamorphism of the snow was sufficiently slow, the field measurements of the liquid water content of snow were achieved every 3 h, from 6 a.m. to midnight.

More specifically, Fig. 2c illustrates the vertical arrangements of the temperature sensor system, which can measure the temperatures from the indoor rooftop (IRT), the roof surface (SRT), the snow at various depths in area B (SLT1 and SLT2) for both central area (with prefix C) and boundary (with prefix B). For comparison, an individual temperature sensor (BRT) was installed in a louver on the bare roof. Besides, two heat flux meters (JZRL-2, Tinel, Inc) were adhered to the indoor rooftop (IRHF) to measure the heat-losses in the snow-covered roof and the bare roof. All measured thermal data was collected at intervals of 1min, the data being downloadable during the field measurement period.

3.2. Prototype boundaries

Based on the classification for international seasonal snow [32], the prototype snow microstructure on the roof surface was mainly in a form of depth hoar. Moreover, since there were no other supplementary precipitations, the overall depth of the snow-layer during this period almost remained the same, about 174 mm. The weather conditions were divided into two categories, one was termed sunny (with adequate direct sunlight in the daytime), the other being cloudy. Four typical days (from January 3 to 6 in 2018), which including both sunny and cloudy conditions, were selected to analyze the heat transfer process in the balanced snow-layer, as shown in

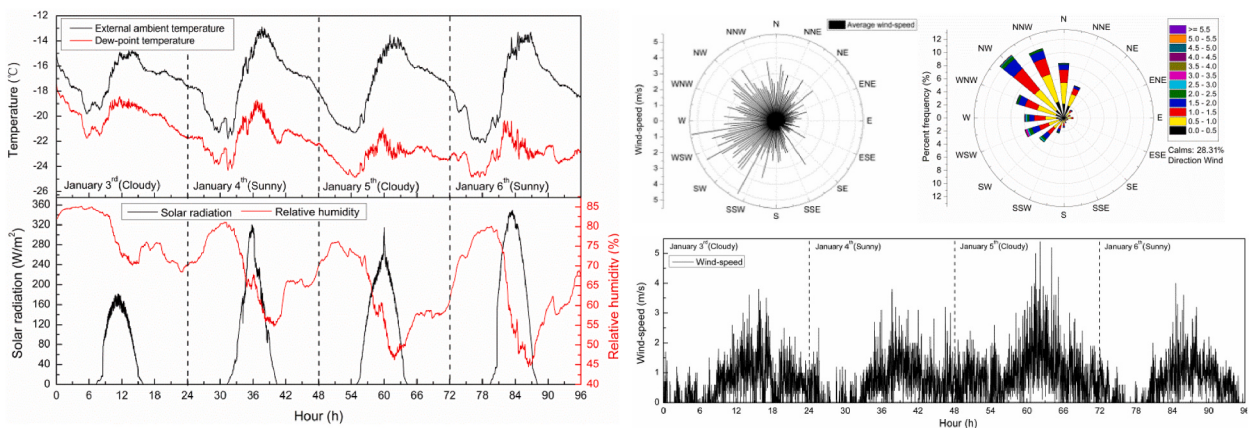


Fig. 3. Meteorological conditions during the measurement period.

Fig. 3.

The air temperature, dew-point temperature, relative humidity, solar radiation, wind speed, and direction were recorded to establish references for the thermal boundary determination in the FEM, especially in the calculations of turbulent exchange and net radiation.

To establish a reasonable empirical evaluation model between snow temperature and density, a series of discontinuous measurements were carried out, and the measured results are shown in Fig. 4a. By using a 1st order polynomial fitting method with 95% confidence bounds, a quantitative relationship between two parameters can be accordingly acquired. In brief, this relation can be active at the low-temperature range, but with the temperature rising, the randomness of density shows a significant increase, this can be attributed to the snow sample discrepancies since the occurrence of local snow metamorphism is caused by solar radiative heat.

As illustrated in Fig. 4b, the measured change of liquid water content in the snow-layers was less than 0.02 vol% during a certain period when the temperature was below -13°C . Thus, its contribution to calculate the volumetric heat enthalpy of snow, according to Eq. (2), can be roughly neglected. However, with temperature and solar radiation intensity rising, the liquid component volume fraction showed a remarkable increasing trend. Likewise, by using a 1st order polynomial fitting method with 95% confidence bounds, an empirical relationship can be set up to calculate snow enthalpy based on its temperature. All those temperature-dependent snow physical properties can constitute a material constitutive model that is used in the subsequent FEM modelling.

4. FEM modelling validation

3.3. Auto-recorded snow-layer temperature

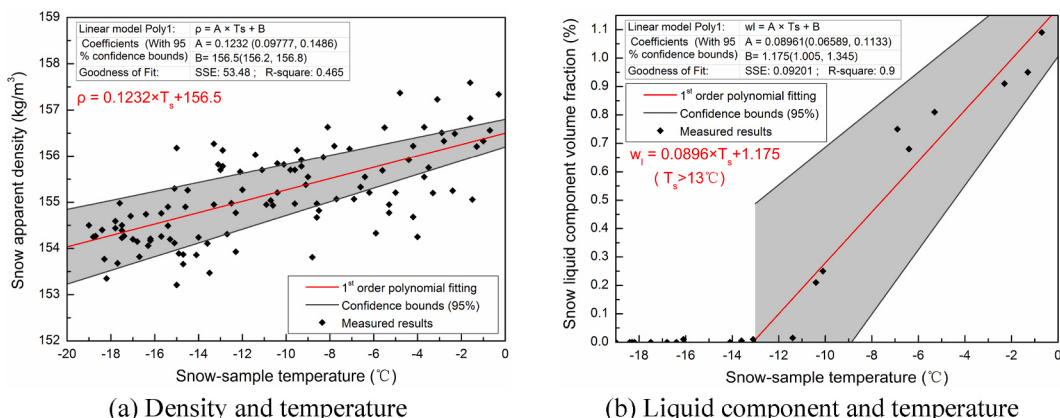
Fig. 5a shows the vertical temperature changes of snow-layer, and it shows that the indoor rooftop temperature with a smooth and steady variation, about 19°C , during the measurement period. The outdoor roof temperatures vary in line with the ambient temperature, but with an obvious difference in the overall temperature variation between the bare roof (BRT) and snow-covered roof (CSRT). Although the sensors, that are buried in the snow, appear to be non-functional for several time intervals, the envelope temperature of CSRT is about 2°C higher than that of BRT on cold nights. And the latter shows a remarkable hysteresis during the daytime warm-up period. In contrast to the internal snow, the snow located at the surface is generally sensitive to the influence of the changing external environment, where the temperature difference can reach about 6.7°C , on average at night, but reverses at noon due to the accumulation of solar radiative heat in the sunny conditions.

As shown in Fig. 5b, the temperature differences in the measured snow-layers were also recorded in the horizontal direction, due to the inconformity of the thermal conditions. The boundary area (BSLT) snow shows more fluctuations at noon than that of the central area (CSLT); particularly in sunny conditions with sufficient turbulent exchange. The measured mean temperature difference in the vertical direction of the central snow (CSLT1 and CSLT2) reaches about 4.3°C , and that for the boundary of the snow-layers (BSLT1 and BSLT2) is only 2.5°C . But the trend of temperature gradient reverses in the latter, at noon, was more obvious for both sunny and cloudy conditions.

4.1. Model establishment

Based on the above-mentioned theories and prototype measurements, a FEM model for simulating hourly heat transfer in a snow-covered building roof was developed in software ANSYS. In detail, the model geometry was the same size as the field site ($3 \times 3 \text{ m}$), where the vertical depth of snow-layer and roof construction were also in accordance with the prototype. The meshes for snow-layer were selected as $0.02 \times 0.02 \text{ m}$ to provide the required resolution. Herein, the SOLID70 element was selected to represent the heat transfer medium, a contact pair (CONTA174, TARGE170) was adhered to the interface of the snow-layers and roof surface to simulate the thermal contact resistance in the heat conduction.

Two thermal properties, including snow and concrete, were initially specified to the corresponding elements, where the snow (depth hoar) element properties were determined based on the regressive analysis of its temperature-dependent constitutive model

**Fig. 4.** Manual measured snow properties.

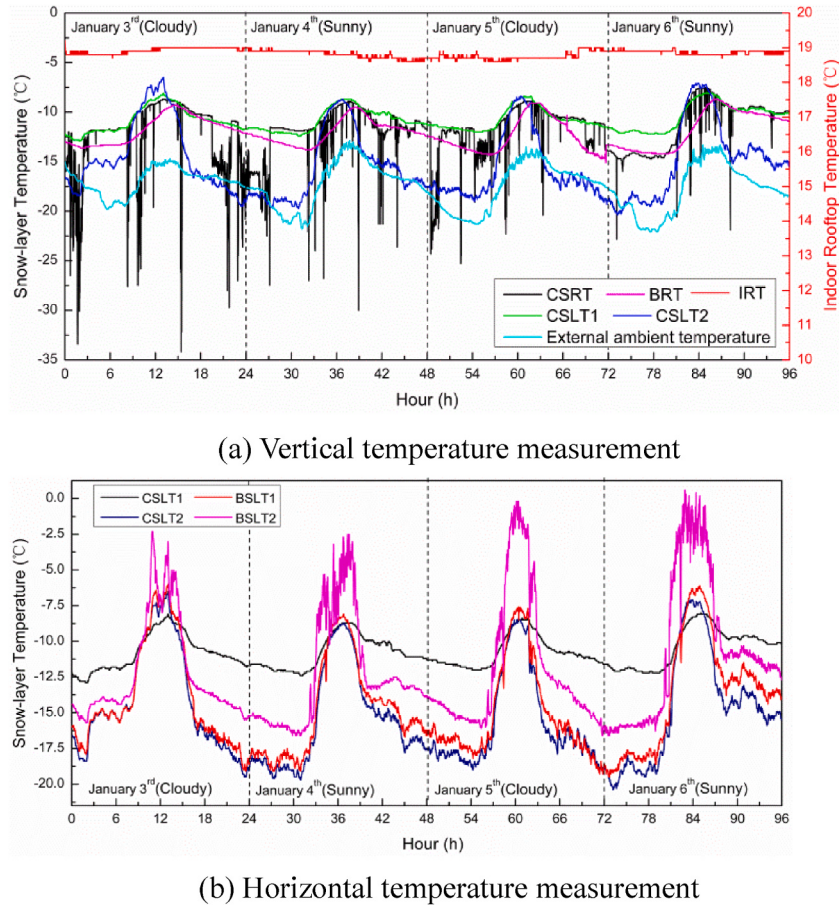


Fig. 5. Temperature variation in the balanced snow-layer on the building roof.

without considering the anisotropy [33]. Moreover, to develop the birth and death element technique, two more element categories (water and ice) were accordingly defined and adopted. In summary, all those parameters used for illustrating the FEM material properties are presented in Table 1.

For the FEM loading history, it can be divided into two steps: 1) the pre-loaded convection heat was applied on the indoor rooftop and snow-layer based on the prototype measurements, primarily to determine the initial boundary conditions for the subsequent loading; and 2) the formal load was applied in the form of multi-steps at intervals of 1 h. More specifically, the snow surfaces were set as the convective boundaries, and the whole snow-layer was also assumed to be a thermogenic volume, where the non-uniform heat generations (equivalent net radiative and convective heats) in vertical direction were applied simultaneously. All applied thermal loads in the formal loading period were previously calculated based on the above-mentioned theories on determining the source-term.

4.2. Model validation

By comparing the qualitative snowmelt phenomena between the FEM and prototype measurement (Fig. 6), it can find that the

Table 1
Inputted FEM modelling parameters.

Numerical model parameters	Temperature (°C)							
	-22	-18	-14	-10	-6	-2	0	2
Snow	Apparent density (kg/m^3)	153.79	154.28	154.78	155.27	155.76	156.25	156.5
	Effective thermal conductivity ($\text{W} \cdot \text{m}^{-1} \cdot {}^\circ \text{C}^{-1}$)	0.0642	0.0645	0.0649	0.0652	0.0655	0.0658	0.0660
	Contact thermal conductivity ($\text{W} \cdot \text{m}^{-1} \cdot {}^\circ \text{C}^{-1}$)	0.0830	0.0833	0.0836	0.0839	0.0841	0.0844	0.0845
	Heat enthalpy ($\times 10^6 \text{J}/\text{m}^3$)	0	2.1	10.5	18.9	27.3	35.7	79.8
Ice/Water/Roof	Specific heat ($\text{J} \cdot \text{kg}^{-1} \cdot {}^\circ \text{C}^{-1}$)	2100						
	Apparent density (kg/m^3)	920/1000/2400						
	Effective thermal conductivity ($\text{W} \cdot \text{m}^{-1} \cdot {}^\circ \text{C}^{-1}$)	2.26/0.551/0.1175						
	Specific heat ($\text{J} \cdot \text{kg}^{-1} \cdot {}^\circ \text{C}^{-1}$)	2260/4200/840						

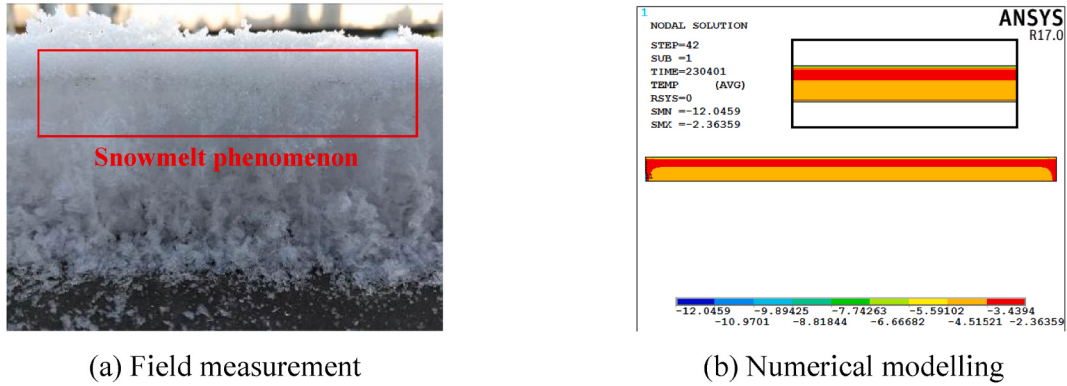


Fig. 6. Result comparisons between the prototype and FEM modelling.

simulated positions of the snowmelt occurrence are in good accordance with the field observation, where the snow geometrical boundaries are relatively sensitive to the ambient temperature fluctuation. Hence, the snowmelt phenomena are more likely to appear in those regions and gradually move to the central area. Especially, the region just beneath the surface is more vulnerable to snow metamorphism under the energy exchange throughout the day.

As shown in Fig. 7a, we take the simulated results of January 6 for example, which has a good interpretation of the heterogeneity in the quantitative snow temperature fluctuation. It can find that the fluctuating temperature amplitude is highly linked to the depth of the central snow-layer (CSLT), and there is a clear reversal in the vertical temperature gradient of snow at noon, where the snow surface temperature is universally 1.7–4.4 °C higher than the internal snow. Notably, the extreme temperature fluctuation is discovered at a position a little below the snow surface, the temperature difference can reach 1.9 °C on average.

By comparing the simulated results with the measured data in some typical regions, as shown in Fig. 7b, it can find that the temperature difference is less than 0.5 °C in the snow interior (CSLT1), and the trend, as well as temperature amplitude, of the snow surface in both central (CSLT2) and boundary (BSLT2) regions are in agreements, although the transient temperature fluctuation can't be depicted due to the homogenizing treating of the airflow. The assumption of treating snow-layer, only for measured depth hoar, as several thermogenic volumes can also have a certain influence on the temperature-fall period (16–18 o'clock), where the simulated cooling rate was lower than that of the prototype.

4.3. Model analysis

Fig. 8 shows the simulated results of several representative hours, like early morning, noon and night, on January 6. Like the prototype, the snow temperature change in the FEM is in accordance with that of ambient temperature. The conductive heat from the underlying roof heat-loss is the main source generating the vertical temperature difference in the snow-layer before sunrise, but the amplitude is not obvious. In contrast, the boundaries of snow-layer show a high sensitivity to the convective heat caused by air flow, where their temperatures are generally 5.9 °C lower than the interior of snow, as shown in Fig. 8a. Then, a steady rise in snow temperature develops until 14 o'clock due to the accumulation of solar radiative heat (Fig. 8b and c), and by this time, in total, the temperature of 644 snow elements (0.32%) can reach the melting point (0 °C). And all those overheated snow elements are located underneath the snow surface, due to the coupling effects of the solar radiation infiltration and surface convective heat exchange.

Subsequently, the heat transfer processes show some significant changes in snow since the newborn of water and ice elements (Fig. 8d), where heat is more likely to concentrate in those new elements with relatively high thermal conductivity. The snow temperature shows a non-linear drop and reaches a minimum at 6 to 7 o'clock on the next day, as illustrated in Fig. 8e and f. On the whole, the influences of turbulent exchange on snow geometrical boundaries can't be ignored, generally, the temperature difference between the snow center and boundaries can even increase with time.

To illustrate the details of the snowmelt simulation, the vertical profiles of snow in some moments were also acquired, as shown in Fig. 9. Based on the FEM results, it can find that the effects of the snowmelt on the heat transfer mechanism are twofold. Firstly, the melting water can transfer more heat to its surroundings, which can cause a remarkable increase the high-temperature areas (Fig. 9d) compared to that in a critical state of snowmelt (Fig. 9c). Those high-temperature areas also increase with time and tend to permeate into the snow gradually under the influence of the heat convection in turbulent exchange. Secondly, the formation of ice-layer in the gap between snow and roof surface can significantly enhance the degree of the heat conduction, so that the amplitude of vertical snow temperature gradient can accordingly increase with time, where the maximum temperature difference reaches about 2.4 °C, as shown in Fig. 9e and f. In essence, the melting and refreezing of snow have an adverse effect on the homogeneity of snow temperature field distribution.

5. Conclusions

To explore the effects of energy exchange (snowmelt) on snow load, different from the existing result-oriented observations, this study provides new insight into the quantified assessment via the FEM modeling of the heat transfer process in snow deposited on the

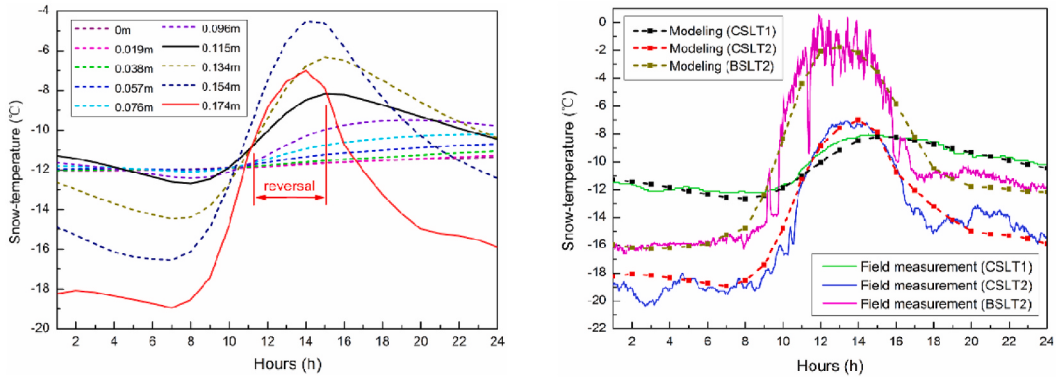


Fig. 7. Quantitative analysis of the simulated results.

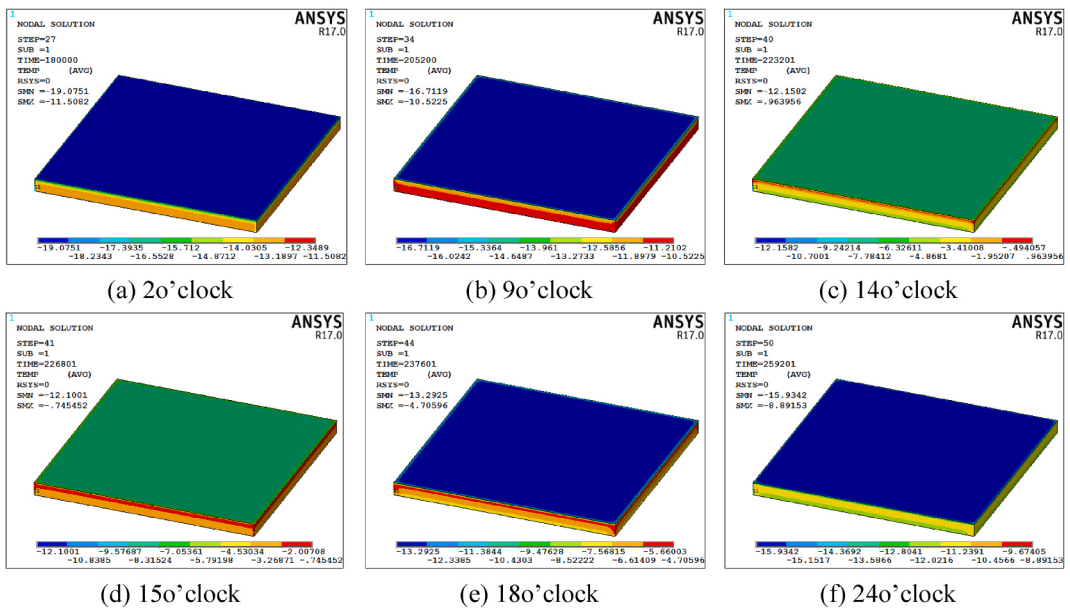


Fig. 8. Simulated results of the snow-layer's temperature distribution.

building roof. According to reasonable modeling strategies, the dynamic change of snow thermal properties in the heat transfer analysis could be visually considered, which differs from the existing FEM of inputting stationary parameters for snow material. In detail, all heat transfer from roof heat-loss conduction, surrounding turbulent exchange and net radiation, as well as the involved phase-changes in snow metamorphism, are calculated. The main conclusions in this study can be drawn as follows.

- 1) Based on a long-term benchmark measurement (case study) on the heat transfer in a snow-covered building roof, the periodicity variety and regional difference in the snow deposited on the building roof have been acquired. In this field observation, the temperature of the roof surface below the snow-layers was about 2 °C higher than the bare roof on a cold night, and the vertical temperature difference between snow surface and interior can be about 6.7 °C, on average at night, and a temperature gradient reversal can occur at noon due to the solar radiation accumulation. The snow geometrical boundaries are relatively sensitive to the ambient temperature fluctuation.
- 2) To achieve the update of snow thermal properties (model parameters) in the heat transfer analysis, a temperature-dependent snow constitutive model, including the determinations of the effective thermal conductivity and the heat enthalpy, has been proposed based on the prototype measurements of snow physical properties, namely the density and the liquid water content.
- 3) To investigate the universality of the proposed snow constitutive model in heat transfer calculation, a FEM modelling was developed using ANSYS. The application of the birth and death element technique can reproduce the snowmelt and subsequent ice-layer formation on the roof surface. The FEM is verified by result comparison, where the largest simulative errors, for the

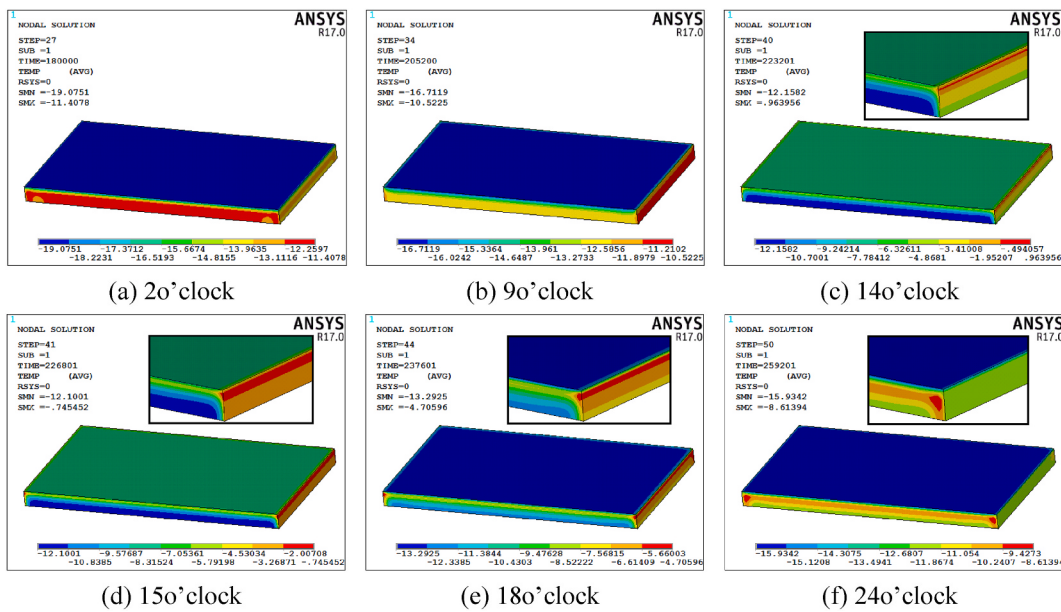


Fig. 9. Vertical profiles of the snow-layer's temperature distribution.

temperature differences, were less than 0.5°C in the snow interior. On the whole, the region just beneath the snow surface was more likely to appear as a potential snowmelt phenomenon, and tended to permeate into the snow gradually with time.

- 4) Compared to the existing 1-D snowmelt models, our new FEM modelling shows a better reproduction of snow temperature distributions. And the visualization of melting and ice-layer formation in the FEM can further illustrate the heat transfer mechanism in the snow, where the melting water and ice-layer can transfer more heat to their surroundings.

The limitation of this study is the limited range of time-scales and the influence of water vapor transport in snow. However, the effort of gathering measurement data for a certain snow category (depth hoar) on its constitutive model, as well as required parameters in the FEM is substantial and will be continued in the future.

Author statement

Conceptualization: Feng Fan.

Methodology: Borui Zhang.

Validation: Borui Zhang and Qingwen Zhang.

Formal analysis: Borui Zhang.

Investigation: Borui Zhang and Huamei Mo.

Resources: Feng Fan.

Data curation: Huamei Mo and Qingwen Zhang.

Writing – original draft: Borui Zhang.

Writing – original draft: Borui Zhang

Visualization: Qingwen Zhang

Supervision: Feng Fan

Project administration: Feng Fan

Project administration: Feng Fan.
Funding acquisition: Qingwen Zheng and Feng Fan.

Declaration of competing interest

The authors declare that they have no known competing financial interests or personal relationships that could have appeared to influence the work reported in this paper.

Acknowledgements

The research funding was provided by the Chinese national natural science fund project (51978207) and the excellent youth foundation of Heilongjiang scientific committee (XQ2021E030).

References

- [1] A. Nielsen, Snow, Ice and Icicles on Roofs – Physics and Risks. 7th Nordic Conference on Building Physics in the Nordic Countries, Reykjavik, Iceland, 2005.
- [2] J. Geis, K. Strobel, A. Liel, Snow-induced building failures, *J. Perform. Constr. Facil.* 26 (4) (2012) 377–388.
- [3] ASCE/SEI 7-16, Minimum Design Loads and Associated Criteria for Buildings and Other Structures, American Society of Civil Engineer, Reston, 2017.
- [4] ISO4355:2013, Bases for Design of Structures – Determination of Snow Loads on Roofs, HIS, Switzerland, 2013.
- [5] R.L. Sack, G.G. Burke, J. Penningroth, Automated data acquisition for structural snow loads, in: Proc. 41st Eastern Snow Conf, 1984. New Carrollton, MD.
- [6] A.M. Baumgartner, R.L. Sack, J.J. Scheldorf, Thermal Characteristics of a Double roof, 1st International Conference on Snow Engineering, 1988. Santa Barbara, California, USA.
- [7] P.A. Irwin, S.L. Gamble, D.A. Taylor, Effects of roof size, heat transfer, and climate on snow loads: studies for the 1995 NBC, *Can. J. Civ. Eng.* 22 (4) (1995) 770–784.
- [8] M. Zhao, J. Srebric, R.D. Berghage, K.A. Dressler, Accumulated snow layer influence on the heat transfer process through green roof assemblies, *Build. Environ.* 87 (2015) 82–91.
- [9] J. Claesson, A. Nielsen, Melting of Snow on a Roof, Department of Civil and Environmental Engineering, Chalmers University of Technology, Goteborg, Sweden, 2011.
- [10] A. Fujimoto, H. Terasaki, T. Fukuhara, A roof snow load model by a heat, ice, water and air balance method, *J. Jap. Soc. Civ. Eng.* 70 (4) (2014) 427–432.
- [11] T.J. L McComb, A.B. Rimmer, M.L.B. Rodgers, et al., A mathematical model for the prediction of temperature in a dry snow lawyer, *Cold Reg. Sci. Technol.* 20 (3) (1992) 247–259.
- [12] L. Zhang, N. Tariq, M.M. Bhatti, E.E. Michaelides, Mixed convection flow over an elastic, porous surface with viscous dissipation: a robust spectral computational approach, *Fractal Fract.* 6 (2022) 263.
- [13] R. Jordan, A one-dimensional temperature model for a snowcover, CRREL Spec. Rep. 91 (1991) 16.
- [14] P. Bartelt, M. Lehning, A physical SNOWPACK model for the Swiss avalanche warning: Part I: numerical model, *Cold Reg. Sci. Technol.* 35 (3) (2002) 123–145.
- [15] M.M. Bhatti, H.F. Öztop, R. Ellahi, I.E. Sarris, M.H. Doranegard, Insight into the investigation of diamond (C) and Silica (SiO_2) nanoparticles suspended in water-based hybrid nanofluid with application in solar collector, *J. Mol. Liq.* 357 (2022), 119134.
- [16] J. Bear, Y. Bechmat, *Introduction to Modeling Transport Phenomena in Porous Media*, Kluwer Academic Publishers, 1991.
- [17] A. Reimer, The effect of wind on heat transfer in snow, *Cold Reg. Sci. Technol.* 3 (2–3) (1980) 129–137.
- [18] C.R. Swaminathan, V.R. Voller, On the enthalpy method, *Int. J. Numer. Method.* 3 (1993) 233–244.
- [19] E.E. Adams, Model for effective thermal conductivity of a dry snow cover composed of uniform ice spheres, *Ann. Glaciol.* 18 (1993) 300–304.
- [20] M. Sturm, J. Holmgren, M. Konig, K. Morris, The thermal conductivity of seasonal snow, *J. Glaciol.* 43 (1997) 26–41.
- [21] F. Riche, M. Schneebeli, Thermal conductivity of snow measured by three independent methods and anisotropy considerations, *Cryosphere* 7 (2013) 217–227.
- [22] M. Cooper, B. Mikic, M. Yovanovich, Thermal contact conductance, *Int. J. Heat Mass Tran.* 12 (1969) 279–300.
- [23] C.W. Fairall, E.F. Bradley, J.E. Hare, A.A. Grachev, J.B. Edson, Bulk parameterization of air-sea fluxes: updates and verification for the COARE Algorithm, *J. Clim.* 16 (2003) 571–591.
- [24] I.S. Bowen, The ratio of heat losses by conduction and evaporation from any water surface, *Phys. Rev.* 27 (1926) 779–787.
- [25] F.P. Incropera, D.P. DeWitt, *Fundamentals of Heat and Mass Transfer*, John Wiley & Sons Inc, 1985.
- [26] W.H. Dilger, A. Ghali, M. Chan, Temperature stresses in composite box girder bridges, *J. Struct. Eng. ASCE.* 109 (6) (1983) 1460–1478.
- [27] J.L. Threlkeld, Solar irradiation of surfaces on clear days, *Build. Eng.* 69 (1963).
- [28] J.C. Giddings, E. LaChapelle, Diffusion Theory applied to radiant energy distribution and albedo of snow, *J. Geophys. Res.* 66 (1) (1961) 181–189.
- [29] R.W. Bliss, Atmospheric radiation near the surface of the earth, *Sol. Energy* 59 (3) (1961) 103–108.
- [30] S. Liu, Y. Huang, Discussion on effective sky temperature, *Acta Energiae Solaris Sin.* 4 (1) (1983) 63–68 ([in Chinese]).
- [31] E. Morris, Field measurement of the liquid-water content of snow, *J. Glaciol.* 27 (95) (1981) 175–178.
- [32] S.C. Colbeck, *Snow Metamorphism and Classification, Seasonal Snowcovers: Physics. Chemistry. Hydrology*, Springer Netherlands, 1987, pp. 1–35.
- [33] M. Sturm, J. Johnson, Thermal conductivity measurements of depth hoar, *J. Geophys. Res. (B2)* (1992) 2129–2139.